Radiative seesaw model: Warm dark matter, collider signatures, and lepton flavor violating signals

PHYSICAL REVIEW D **79,** 013011 (2009)

Radiative seesaw model: Warm dark matter, collider signatures, and lepton flavor violating signals

D. Aristizabal Sierra
INFN, Laboratori Nazionali di Frascati, C.P. 13, I00044 Frascati, Italy

Jisuke Kubo and Daijiro Suematsu
Institute for Theoretical Physics, Kanazawa University, 920-1192 Kanazawa, Japan

D. Restrepo and Oscar Zapata*
Instituto de Física, Universidad de Antioquia, A.A.1226, Medellín, Colombia
(Received 8 September 2008; published 28 January 2009)

Extending the standard model with three right-handed neutrinos (N_k) and a second Higgs doublet (η), odd under the discrete parity symmetry Z_2, Majorana neutrino masses can be generated at one-loop order. In the resulting model, the lightest stable particle, either a boson or a fermion, might be a dark matter candidate. Here we assume a specific mass spectrum ($M_1 \ll M_2 < M_3 < m_\eta$) and derive its consequences for dark matter and collider phenomenology. We show that (i) the lightest right-handed neutrino is a warm dark matter particle that can give a $\sim$10% contribution to the dark matter density; (ii) several decay branching ratios of the charged scalar can be predicted from measured neutrino data. Especially interesting is that large lepton flavor violating rates in muon and tau final states are expected. Finally, we derive upper bounds on the right-handed neutrino Yukawa couplings from the current experimental limit on $Br(\mu \to e\gamma)$.

DOI: 10.1103/PhysRevD.79.013011 PACS numbers: 14.60.Pq, 12.60.Fr, 13.15.+g, 14.60.St

I. INTRODUCTION

Solar [1], atmospheric [2], and reactor [3] neutrino experiments have demonstrated that neutrinos have mass and nonzero mixing angles among the different generations. On the other hand, observations of the cosmic microwave background, primordial abundances of light elements, and large scale structure formation have firmly established that most of the mass of the Universe consists of dark matter (DM) [4]. These experimental results are at present the most important evidences for physics beyond the standard model.

There are several ways in which neutrino masses can be generated. Certainly the best-known mechanism to generate small Majorana neutrino masses is the seesaw [5]. However, a large variety of models exists in which lepton number is broken near or at the electroweak scale. Examples are supersymmetric models with explicit or spontaneous breaking of R parity [6,7], models with Higgs triplets [8], pure radiative models at one-loop [9] or at two-loop [10] order, and models in which neutrino masses are induced by leptoquark interactions [11].

According to their free-streaming length, DM particle candidates can be classified as either hot, warm, or cold DM. Because of their large free-streaming length, the mass and density of hot DM particles are strongly constrained [12,13]. Contrary, cold DM particles have a free-streaming length which is irrelevant for cosmological structure formation. Actually, cold DM is usually considered the best choice to fit large scale structure data [14]. Warm DM (WDM) particles, for instance those that decouple very early from the thermal background, have a smaller temperature than that of hot dark matter relics and thus a shorter free-streaming length.

It has been argued in the literature [15] that WDM scenarios may be able to overcome the shortcomings of the standard cold DM scenario. Constraints on WDM particles have been quoted in Ref. [16]. If DM consists only of WDM, $m_{\rm WDM} \gtrsim 1.2$ keV whereas in mixed scenarios, in which the DM relic density receives contributions from cold and WDM as well, $m_{\rm WDM} \lesssim 16$ eV [17].

The question of whether neutrino mass generation and DM are related has lead to a large number of models [18]. In this paper we focus on a particular realization, namely the radiative seesaw model [19]. In this scheme three right-handed neutrinos N_i and a second Higgs doublet $\eta = (\eta^+, \eta^0)$, odd under the discrete parity symmetry Z_2, are added to the standard model. As a result (a) the new Higgs doublet has a zero vacuum expectation value and there is no Dirac mass term. Thus, neutrinos remain massless at tree level; (b) the lightest particle in the spectrum, either a boson or a fermion, is stable and therefore, in principle, can be a dark matter candidate [20].

Here we study the implications for DM and possible collider signatures of this model. Our analysis is done in a particular scenario in which the Yukawa couplings of N_3 are larger than those from N_2 and the right-handed neutrino

*Also at Escuela de Ingeniería de Antioquia, Calle 25 sur No. 42-73, Envigado, Colombia.

spectrum is such that $M_1 \ll M_2 < M_3$. The right-handed neutrinos are assumed to be always lighter than the charged and neutral scalars. As it will be shown, the lightest neutrino singlet cannot be a cold DM candidate and instead behaves as WDM, contributing with less than 10% to the total DM relic density. In addition we will show that current experimental neutrino data enforces a number of constraints on the parameter space of the model. These constraints, in turn, can be used to predict the decay patterns of the charged scalar $\eta^{\pm}$. Therefore, the hypothesis that this model is responsible for the generation of neutrino masses (within our scenario) and that N_1 is a WDM particle can be tested in collider experiments.

The rest of this paper is organized as follows: in Sec. II we briefly describe the model, paying special attention to the neutrino mass generation mechanism. In Sec. III we present simple and useful analytical results for neutrino masses and mixing angles. In Sec. IV we discuss dark matter within the model and show that the lightest right-handed neutrino is a WDM relic. We then turn to the collider phenomenology of charged scalars in Sec. V. We show that different ratios of branching ratios of $\eta^{\pm}$ can be predicted from measured neutrino mixing angles. In Sec. VI we analyze the implications of the model for lepton flavor violating decays, in particular for $\mu \to e\gamma$. Finally in Sec. VII we present our conclusions.

II. NEUTRINO MASS GENERATION

The model we consider [19] is a simple extension of the standard model, containing three $SU(2)_L \times U(1)_Y$ fermionic singlets N_i and a second Higgs doublet η. In addition, an exact Z_2 discrete symmetry is assumed such that the new fields are odd under Z_2, whereas the standard model fields are even. The Yukawa interactions induced by the new Higgs doublet are given by

$$\mathcal{L} = \epsilon_{ab} h_{\alpha j} \bar{N}_j P_L L^a_\alpha \eta^b + \text{H.c.} \tag{1}$$

Here, L are the left-handed lepton doublets, α, j are generation indices (Greek indices label lepton flavor e, μ, τ), and ϵ_{ab} is the completely antisymmetric tensor. Apart from these Yukawa interactions the quartic scalar term

$$\tfrac{1}{2}\lambda_5(\phi\eta)^2, \tag{2}$$

where ϕ is the standard model Higgs doublet, is also relevant for neutrino mass generation. Since Z_2 is assumed to be an exact symmetry of the model η has zero vacuum expectation value. Thus, there is no mixing between the neutral CP-even (CP-odd) components of the Higgs doublets. The physical scalar bosons are, therefore, Re ϕ^0, $\eta^{\pm}$, $\eta^0_R \equiv$ Re η^0, and $\eta^0_I \equiv$ Im η^0.

The setup of Eqs. (1) and (2) generates Majorana neutrino masses through the diagram shown in Fig. 1. The resulting neutrino mass matrix can be written as

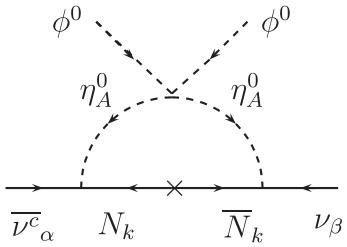

FIG. 1. Feynman diagram for Majorana neutrino masses. $A = R, I$ labels the contributions from the neutral CP-even and CP-odd components of the Higgs doublet η.

$$(\mathcal{M}_\nu)_{\alpha\beta} = \frac{1}{16\pi^2} \sum_{\substack{A=I,R \\ k=1\ldots3}} c_A M_k h_{\alpha k} h_{\beta k} B_0(0, m_A^2, M_k^2). \tag{3}$$

Here $A = R, I$, M_k are the right-handed neutrino masses, m_A are the η^0_A masses, $c_R = +1$ while $c_I = -1$, and $B_0(0, m_A^2, M_k^2)$ is a Passarino-Veltman function [21]. The function B_0 has a finite and an infinite part. Note that the infinite part cancels after summing over A and the resulting formula can be expressed as a *difference* of two B_0 functions. The finite part of the Passarino-Veltman function B_0^f is given by

$$B_0^f(0, m_A^2, M_k^2) = \frac{m_A^2 \log(m_A^2) - M_k^2 \log(M_k^2)}{m_A^2 - M_k^2}. \tag{4}$$

As pointed out in Ref. [19] if η_R and η_I are almost degenerate, i.e. $m_R^2 - m_I^2 = 2\lambda_5 v^2$ [$v^2 = (2\sqrt{2}G_F)^{-1}$] is assumed to be small compared to $m_0^2 = (m_R^2 + m_I^2)/2$, the neutrino mass matrix in (3) can be rewritten as

$$(\mathcal{M}_\nu)_{\alpha\beta} = \frac{\lambda_5 v^2}{8\pi^2} \sum_{k=1\ldots3} \frac{h_{\alpha k} h_{\beta k} M_k}{m_0^2 - M_k^2} \times \left[1 - \frac{M_k^2}{m_0^2 - M_k^2} \log\left(\frac{m_0^2}{M_k^2}\right)\right]. \tag{5}$$

Depending on the relative size between m_0 and M_k, this formula can be simplified [19]. Here we will focus on the limiting case $m_0^2 \gg M_k^2$.

III. ANALYTICAL RESULTS

Here we will consider a right-handed neutrino spectrum such that $M_1 \ll M_2 < M_3$. In addition, as previously mentioned, we will also consider the limiting case $m_0^2 \gg M_k^2$. In this case the neutrino mass matrix in Eq. (5) becomes

$$(\mathcal{M}_\nu)_{\alpha\beta} = \frac{\lambda_5 v^2}{8\pi^2 m_0^2} \sum_{k=1\ldots3} h_{\alpha k} h_{\beta k} M_k. \tag{6}$$

In general, the neutrino mass matrix receives contributions from diagrams involving the three right-handed neutrinos. However, if N_1 is light enough, let us say, $\mathcal{O}(M_1/M_2) < 10^{-2}$, the contributions from N_1 become negligible. In this limit $\det[\mathcal{M}_\nu] \simeq 0$ and therefore only two neutrinos have

nonzero masses. In this case simple analytical formulas involving neutrino mixing angles and Yukawa couplings can be derived. Note that in this limit only a hierarchical spectrum is possible. In what follows we will focus on the normal spectrum. Some comments on the inverted one will be given in Sec. V B.

In the limit $\det[\mathcal{M}_\nu] \simeq 0$ the mass matrix structure is determined by the Yukawa couplings $h_{\alpha(2,3)}$. Therefore, it is useful to define two vectors in parameter space:

$$\mathbf{h_2} = (h_{12}, h_{22}, h_{32}), \qquad \mathbf{h_3} = (h_{13}, h_{23}, h_{33}). \tag{7}$$

In terms of these vectors the two nonzero neutrino masses can be written as

$$m_{\nu_{2,3}} = \mathcal{G}_f\left[1 \mp \sqrt{1 - 4r_N \frac{|\mathbf{h_2}|^2|\mathbf{h_3}|^2 - |\mathbf{h_2}\cdot\mathbf{h_3}|^2}{(r_N|\mathbf{h_2}|^2 + |\mathbf{h_3}|^2)^2}}\right], \tag{8}$$

where $\mathcal{G}_f$ is given by

$$\mathcal{G}_f = \frac{\lambda_5 v^2 M_3}{16\pi^2 m_0^2}(r_N|\mathbf{h_2}|^2 + |\mathbf{h_3}|^2) \tag{9}$$

and

$$r_N = \frac{M_2}{M_3}. \tag{10}$$

The ratio between the solar and the atmospheric scale is approximately given by

$$R \equiv \sqrt{\frac{\Delta m_{21}^2}{\Delta m_{32}^2}} \simeq \frac{m_{\nu_2}}{m_{\nu_3}}. \tag{11}$$

Thus, from Eqs. (8) and (9), it can be noted that R is independent of $\mathcal{G}_f$ and therefore independent of λ_5 and m_0.

The generation of the nonzero lightest neutrino mass can be understood from the misalignment angle between the parameter space vectors $\mathbf{h_{2,3}}$ ($\cos\theta = \mathbf{h_2}\cdot\mathbf{h_3}/|\mathbf{h_2}||\mathbf{h_3}|$) which, from Eq. (8), can be written as

$$\sin^2\theta = \frac{(1 + h_r r_N)^2}{4h_r r_N}\left[1 - \left(\frac{1 - R}{1 + R}\right)^2\right], \tag{12}$$

where $h_r = |\mathbf{h_2}|^2/|\mathbf{h_3}|^2$. Note that since h_r as well as r_N are positive quantities a complete alignment between $\mathbf{h_2}$ and $\mathbf{h_3}$ ($\sin\theta = 0$) is only possible if $R = 0$. However, this possibility is excluded as it implies $m_{\nu_2} = 0$.

There is a minimum value of $\sin^2\theta$ consistent with the experimentally measured values of R. This value is determined by

$$\begin{aligned}\sin^2\theta|_{\min} &= \frac{(1 + h_r r_N)^2}{4h_r r_N}\Big|_{\min}\left[1 - \left(\frac{1 - R}{1 + R}\right)^2\right]_{\min} \\ &= 1 - \left(\frac{1 - R_{\min}}{1 + R_{\min}}\right)^2,\end{aligned} \tag{13}$$

and corresponds to the minimum misalignment between $\mathbf{h_2}$ and $\mathbf{h_3}$. Thus, in order to reproduce the correct solar and atmospheric mass scale ratio $\sin^2\theta \gtrsim 0.47$. Figure 2 shows the misalignment allowed region.

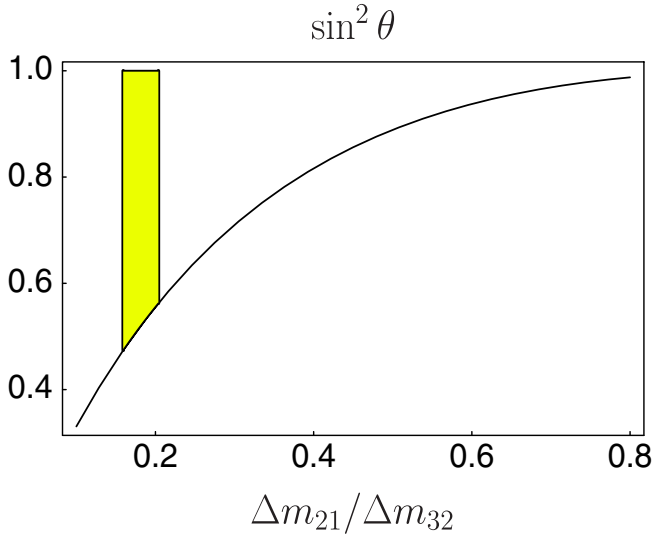

FIG. 2 (color online). The allowed range of the misalignment between the vectors $\mathbf{h_2}$ and $\mathbf{h_3}$.

Although not consistent with neutrino experimental data, there is an interesting limit when the contribution from N_2 to the neutrino mass matrix is small in comparison with those from N_3. In this case the neutrino mass matrix becomes projective and therefore it can be diagonalized with only two rotations. The rotation angles can be written as

$$\tan\theta_{23} = -\frac{h_{23}}{h_{33}}, \qquad \tan\theta_{13} = -\frac{h_{13}}{\sqrt{h_{23}^2 + h_{33}^2}}. \tag{14}$$

As it will be shown in Sec. V, these results are good approximations in the case we are considering.

IV. FERMIONIC DARK MATTER

Before discussing possible collider signals of the charged scalar [22], we will study the implications of the assumed mass spectrum, $M_1 \ll M_2 < M_3 < m_\eta$, on DM. In Ref. [20], N_1 was assumed to be a cold DM particle. Based on this assumption, two crucial observations, related with m_η and the Yukawa couplings $h_{\alpha 1}$, were made:

(i) The following relation has to be satisfied in order to obtain the observed DM relic density, $\Omega_d h^2 \simeq 0.12$ [4]:

$$\left[\sum_{\alpha,\beta}|h_{\alpha 1}h_{\beta 1}^*|^2\right]^{1/2} \gtrsim 0.08\left(\frac{m_\eta}{100\ \text{GeV}}\right)^2. \tag{15}$$

Restricting the Yukawa couplings to the perturbative regime, i.e. the left-hand side of (15) $\lesssim 1$, it was found that $m_\eta \lesssim 350$ GeV. Furthermore, the constraint (15), being a lower bound for the Yukawa couplings $h_{\alpha 1}$, should be compared with the con-

straint derived from $\mu \to e\gamma$, which gives an upper bound for the Yukawa couplings [see Sec. VI, Eq. (42)]. The apparent contradiction between these bounds was overcome by assuming a specific structure for the Yukawa couplings in Ref. [20].

(ii) The constraint $M_1 \gtrsim 10$ GeV for $m_\eta \gtrsim 100$ GeV must be satisfied in addition to the requirement that $M_1 < m_\eta$.

If (i) and (ii) are combined, the hierarchical mass relation $M_1/M_2 < O(10^{-2})$ implies that $M_{2,3} > m_\eta$ which is not consistent with the analysis of neutrino masses discussed in the previous section. Moreover, this relation, in turn, requires another suppression mechanism for $\mu \to e\gamma$ [23]. Therefore, the assumed mass spectrum, $M_1 \ll M_2 < M_3 < m_\eta$, does not fit within the cold DM scenario of [20].

In what follows we will discuss whether N_1 can be a viable WDM candidate. In this case there are important differences compared with the conventional sterile neutrino WDM scenario in which sterile neutrinos are produced by nonresonant active-sterile neutrino oscillations [25,26], namely:

(a) The decay of N_1 is forbidden by the Z_2 symmetry [27]. Thus, the x-ray constraint [28–31], derived from the absence of detection of x-ray photons from sterile neutrino radiative decays, cannot be applied. This constraint, when applied to the conventional sterile neutrino WDM scenario, yields an upper bound of $m_{\rm WDM} \lesssim 4$ keV [31]. This result combined with the Lyman-alpha forest data, which lead to a lower limit of $m_{\rm WDM} \gtrsim 10$–14 keV, has ruled out the possibility [32] that all the DM consists of sterile neutrinos [34,35] (see also [36]).

(b) In the conventional scenario the Yukawa couplings of the right-handed neutrino are tiny. Actually they cannot be thermalized without mixing with the active neutrinos [25] and therefore cannot be regarded as thermal relics. In contrast to the conventional case, the Yukawa couplings $h_{\alpha k}$ in the current model are not necessarily small (see Sec. VI). Thus, N_1 can be in thermal equilibrium at high temperatures. This implies that the constraints discussed in the literature on thermal WDM particles [12,16,34,35] can be applied in our case. Of course, the largest value of $h_{\alpha k}$ must be consistent with the upper bound derived from $\mu \to e\gamma$ [see Eq. (42)].

Current cosmological data constraints [12,16,34,35] imply that DM can consist of only N_1 if the relativistic degrees of freedom at the decoupling temperature [$g_*(T_D)$] are larger than 10^3, for $M_1 \lesssim 1$ keV [16]. This is not satisfied in this model, the relativistic degrees of freedom can be at most 116. Therefore, N_1 can be regarded as WDM if there exists, in addition to N_1, a dominant cold DM relic that gives a contribution of $\sim$90% to the total DM relic density and if $M_1 \lesssim 16$ eV [16] (this possibility, within the conventional WDM sterile neutrino scenario, has been throughout studied in [37]).

From a more detailed analysis of this scenario we have found that the annihilation rate of N_1 at temperature T can be written as

$$\Gamma[T] \simeq \left(\frac{7}{120}\right)^2 \frac{\pi^5}{54\zeta(3)} T^5 \frac{y_1^2}{m_\eta^4}, \qquad y_1^4 \equiv \sum_{\alpha,\beta} |h_{\alpha 1} h_{\beta 1}^*|^2. \tag{16}$$

Here we have assumed $m_\eta \gg T \gg M_1$. The decoupling temperature can be estimated by equating the annihilation rate with the expansion rate, $H = 1.66\sqrt{g_*(T)}T^2/m_{pl}$. From $H(T_D) \simeq \Gamma(T_D)$ we get

$$y_1 \left(\frac{100\ \text{GeV}}{m_\eta}\right)^2 \simeq 3.73 \times 10^{-5} \left(\frac{g_*(T_D)}{g_*(T_\nu)}\right)^{1/4} \left(\frac{\text{GeV}}{T_D}\right)^{3/2}, \tag{17}$$

where T_ν is the decoupling temperature of the active neutrinos and $g_*(T_\nu) = 10.75$. For $T_D \simeq 2$ GeV, for which $g_*(T_D) = 77.5$ [38], Eq. (17) becomes

$$y_1 \left(\frac{100\ \text{GeV}}{m_\eta}\right)^2 \simeq 2.2 \times 10^{-5}, \tag{18}$$

which, as we can see from Eq. (42), satisfies the constraint coming from $\mu \to e\gamma$. Note that a stringent experimental upper limit on $Br(\mu \to e\gamma)$ will imply a larger decoupling temperature. For example, a 3 orders of magnitude more stringent bound on $Br(\mu \to e\gamma)$, as the one expected in near future experiments [39], will enforce T_D to be larger than $\sim$140 GeV.

V. COLLIDER PHYSICS

The Yukawa couplings that govern neutrino physics also determine the fermionic two-body decays of $\eta_{R,I}^0$ and $\eta^\pm$. According to the Yukawa interactions in (1), possible decays of these states are

$$\eta_{R,I}^0 \to \nu_\alpha N_i \tag{19}$$

$$\eta^\pm \to \ell_\alpha^\pm N_i. \tag{20}$$

As will be discussed below, $N_{2,3}$ follow decay chains that can lead to only missing energy. In that case the observation of the neutral Higgses $\eta_{R,I}^0$ will be problematic. On the contrary, since charged scalar final states always contain—at least—a charged lepton their decays are easier to observe. Therefore, we will focus on charged Higgs decays. Apart from the Yukawa interactions the scalar doublet η has also gauge (and scalar) interactions which induce the decays $\eta^\pm \to \eta_{R,I}^0 W^\pm$, if kinematically possible.

At LHC charged scalars can be produced either in association with a neutral scalar (single production) or in pairs [40]. In the former case the mechanism proceeds via

$q\bar{q}$ annihilation mediated by a virtual W vector boson, whereas in the latter case through s-channel exchange of a virtual γ and a Z:

$$q\bar{q} \to \eta^{\pm}\eta^{0}_{R,I} \tag{21}$$

$$q\bar{q} \to \eta^{+}\eta^{-}. \tag{22}$$

Charged scalar production in association with an η^0_I has been calculated in Ref. [41]. According to this result, the production cross section is larger than 100 fb for $m_\eta \lesssim 200$ GeV. The pair production cross section, on the other hand, is further suppressed as it cannot exceed 10 fb for charged scalar masses below 250 GeV [40]. Contrary, at ILC the pair production cross section is larger than 10 fb for $m_\eta \lesssim 350$ GeV [42]. Thus, depending on the accumulated luminosity, LHC (ILC) should be able to explore up to masses of order $m_\eta \sim 200$–250 GeV (400 GeV).

A. Right-handed neutrinos: Decays, signals, and identification

The correlations between charged scalar decays and neutrino mixing angles which will be discussed latter could be studied in collider experiments only if the decaying right-handed neutrino can be identified. Experimentally, in principle, this can be done. Let us discuss this in more detail: right-handed neutrinos, stemming from charged scalar decays, will produce, via an off-shell $\eta^{\pm}$, charged leptons through the decay chains

$$N_3 \to \ell^{\pm}_{\alpha}\eta^{\mp} \to \ell^{\pm}_{\alpha}\ell^{\mp}_{\beta}N_2 \to \ell^{\pm}_{\alpha}\ell^{\mp}_{\beta}\ell^{\pm}_{\alpha'}\eta^{\mp} \to \ell^{\pm}_{\alpha}\ell^{\mp}_{\beta}\ell^{\pm}_{\alpha'}\ell^{\mp}_{\beta'}N_1 \tag{23}$$

$$N_{3,2} \to \ell^{\pm}_{\alpha}\eta^{\mp} \to \ell^{\pm}_{\alpha}\ell^{\mp}_{\beta}N_1. \tag{24}$$

In addition to these decay chains there are others which involve neutral scalars and lead to either dilepton + missing energy ($\ell^{\pm}_{\alpha}\ell^{\mp}_{\beta}\nu_{\alpha'}\nu_{\beta'}N_1$) or missing energy ($\nu_\alpha\nu_\beta\nu_{\alpha'}\nu_{\beta'}N_1$ or $\nu_\alpha\nu_\beta N_1$) signals.

The most important signatures for the identification procedure are (23) and (24) due to their low backgrounds [43]. The right-handed neutrino identification from the remaining decay chains might be rather hard as they involve additional missing energy. Thus, in general, they will diminish the relevant signals. Whether the decay branching ratios for the processes in (23) and (24) can dominate depend upon the different parameters (mainly Yukawa couplings and scalar masses), which we will now discuss in turn. The decay chains in Eq. (23) dominate over the processes $N_3 \to \ell^{\pm}_{\alpha}\ell^{\mp}_{\beta}\nu_{\alpha'}\nu_{\beta'}N_1$ and $N_3 \to \nu_\alpha\nu_\beta\nu_{\alpha'}\nu_{\beta'}N_1$ as long as

$$\sum_{\substack{\alpha,\beta\\ \alpha',\beta'}} Br(N_3 \to \ell^{\pm}_{\alpha}\ell^{\mp}_{\beta}\ell^{\pm}_{\alpha'}\ell^{\mp}_{\beta'}N_1) > \begin{cases} \sum\limits_{\substack{\alpha,\beta\\ \alpha',\beta'}} Br(N_3 \to \ell^{\pm}_{\alpha}\ell^{\mp}_{\beta}\nu_{\alpha'}\nu_{\beta'}N_1) \\ \sum\limits_{\substack{\alpha,\beta\\ \alpha',\beta'}} Br(N_3 \to \nu_\alpha\nu_\beta\nu_{\alpha'}\nu_{\beta'}N_1). \end{cases} \tag{25}$$

The conditions on the parameter space of the model for which (25) is fulfilled can be entirely determined from the three-body decay processes $N_i \to \ell^{\pm}_{\alpha}\ell^{\mp}_{\beta}N_j$ and $N_i \to \nu_\alpha\nu_\beta N_j$ as the branching ratios in (25) are given by

$$\sum_{\substack{\alpha,\beta\\ \alpha',\beta'}} Br(N_3 \to f_\alpha f_\beta f'_{\alpha'} f'_{\beta'} N_1) = \sum_{\substack{\alpha,\beta\\ \alpha',\beta'}} Br(N_3 \to f_\alpha f_\beta N_2) \times Br(N_2 \to f'_{\alpha'} f'_{\beta'} N_1). \tag{26}$$

Thus, from Eq. (26) and using the shorthand notation

$$Br(N_i \to N_j) = \sum_{\alpha,\beta} Br(N_i \to \ell^{\pm}_{\alpha}\ell^{\mp}_{\beta}N_j), \tag{27}$$

$$Br_{\rm inv}(N_i \to N_j) = \sum_{\alpha,\beta} Br(N_i \to \nu_\alpha\nu_\beta N_j), \tag{28}$$

the constraints in (25) become

$$\begin{aligned} Br(N_2 \to N_1) &> Br_{\rm inv}(N_2 \to N_1) \\ Br(N_3 \to N_2) \times Br(N_2 \to N_1) &> Br_{\rm inv}(N_3 \to N_2) \\ &\quad \times Br_{\rm inv}(N_2 \to N_1). \end{aligned} \tag{29}$$

Similar conditions can be also obtained in the case of the decay chains in (24), namely

$$Br(N_i \to N_j) > Br_{\rm inv}(N_i \to N_j). \tag{30}$$

The partial decay width for the process $N_i \to f_\alpha f_\beta N_j$ summed over all possible final states for a fixed j is given by

$$\sum_{\alpha,\beta}\Gamma(N_i \to f_\alpha f_\beta N_j) = \frac{|\mathbf{h}_i|^2|\mathbf{h}_j|^2 + (\mathbf{h}_i\cdot\mathbf{h}_j)^2}{384\pi^3}\frac{M_j^5}{m_S^4} I(M_i/M_j), \tag{31}$$

where

$$I(x) = 1 - 8x^2 - 24x^4\ln(x) + 8x^6 - x^8 \tag{32}$$

and $S = \eta$ if $f = \ell$ or $S = \eta_{R,I}$ if $f = \nu$. This expression, in addition to the conditions (29) and (30), lead to the

constraint

$$m_{\eta_{R,I}} > m_{\eta}. \tag{33}$$

Consequently, as long as the neutral scalars become heavier than the charged one the decay processes in (23) and (24) become dominant. Note that this result holds only if $N_{2,3}$ decay inside the detector. Whether this is indeed the case depends on the parameters that define Eq. (31). Since right-handed neutrino masses $M_{2,3}$ as well as the parameter space vectors $|\mathbf{h_{2,3}}|$ are bounded by neutrino physics, once the constraint (33) is imposed [44] the only free parameter is $\mathbf{h_1}$. Accordingly, the right-handed neutrino decay lengths are strongly determined by the value of $|\mathbf{h_1}|$. We calculate N_2 and N_3 decay lengths by randomly varying the Yukawa couplings $h_{\alpha i}$ for the benchmark point $m_{R,I} = 140$ GeV, $m_{\eta} = 150$ GeV, $M_2 = 25$ GeV, and $M_3 = 45$ GeV. After imposing neutrino physics constraints at the 1σ level [45] we get

$$L_2 \subset [0.08, 300] \text{ m}, \qquad L_3 \subset [10^{-3}, 2] \text{ m}, \tag{34}$$

which shows that N_3 always decay within the detector whereas N_2 decays might occur outside.

As can be seen from Eq. (31) the larger (smaller) $|\mathbf{h_1}|$ the smaller (larger) L_2. For the benchmark point we have considered, it has been found that, in those regions of parameter space in which L_2 is smaller than a few meters, $Br(N_3 \to N_2) \sim \mathcal{O}(10^{-2})$ which implies that most N_3 decays will proceed through the decay chains in (24). On the contrary, when L_2 is large N_2 will behave, from the collider point of view, as N_1 and the only possible signals will be either dilepton + missing energy or missing energy. In this case according to our results the process $N_3 \to \ell_{\alpha}^{\pm}\ell_{\beta}^{\mp}N_1$ will be sizable [$Br(N_3 \to N_1) > 0.1$].

In general, since from Eq. (31) we have

$$Br(N_2 \to N_1) = \frac{m_{R,I}^4}{m_{R,I}^4 + m_{\eta}}, \tag{35}$$

if $m_{\eta} \ll m_{R,I}$ small values of $|\mathbf{h_1}|$ will enhance the decays in (23). For the smallest value of $|\mathbf{h_1}|$ for which N_2 still decays inside the detector (typically 10^{-3}), we found that

$$Br(N_3 \to N_2) \times Br(N_2 \to N_1) \lesssim 0.5. \tag{36}$$

Hard leptons with missing energy [Eqs. (23) and (24)] are typical accelerator signatures in conserving and nonconserving R-parity violating supersymmetric models [43,46]. Indeed, as pointed out in Refs. [43,46], the discovery of supersymmetry could arise from such a signal. In the present case the possibility of having in addition displaced vertices might facilitate the reconstruction of N_2 and N_3. Actually, since W and Z leptonic decay modes occur at the interaction point, these types of signals are practically background-free once the dilepton invariant mass distribution from the displaced vertex is above 10 GeV [43].

Regarding the identification procedure if N_3 decay according to (23), the identification might be possible by counting the number of leptons emerging from a given vertex. In contrast to the decay chain (23), if N_3 follows the processes in (24) the number of leptons from $N_{3,2}$ decays will be the same, and the charged lepton counting "method" cannot be used. In this case N_3 from N_2 decays can be distinguished by looking to the kinematic end point of the lepton pair invariant mass distribution. This method has been extensively discussed in the minimal supersymmetric standard model context [47] and might be also applicable in this case. Note that the kinematic end point technique could be also applicable when N_3 follows the decay chain (23). Thus, the right-handed neutrino identification procedure can be entirely based on this method.

B. Collider signals related to neutrino physics

The results presented below were obtained by numerically diagonalizing Eq. (5) for random parameters and checking for consistency with experimental neutrino constraints [45]. Different correlations among neutrino mixing angles and charged scalar decay branching ratios were found as expected from Eq. (14). The parameter m_0, which essentially corresponds to m_R or m_I, was taken in the range 100 GeV $\leq m_0 \leq$ 400 GeV [48], whereas the masses of N_3 and N_2 between 40 GeV $\leq M_3 \leq$ 50 GeV and 20 GeV $\leq M_2 \leq$ 30 GeV [49]. The Yukawa couplings were chosen such that $|\mathbf{h_2}|/|\mathbf{h_3}| \subset [0.4, 0.9]$. In regions of parameter space in which N_3 and N_2 are comparable—though lighter—to m_{η} the correlations, discussed below, are less pronounced. However, the decay chains [see Eqs. (23) and (24)] will involve hard leptons from which the right-handed neutrinos can be readily identified. On the other hand, if N_3 and N_2 are much lighter than $\eta^{\pm}$ the data points become strongly correlated. In this case, in contrast to the previous one, charged leptons emerging from the decay chains might be near the τ—and possibly μ—threshold which will render the right-handed neutrino identification problematic.

Figure 3 shows that the ratio of decay branching ratios $Br_{\eta^{\pm}}^{\mu N_3}/Br_{\eta^{\pm}}^{\tau N_3}$ ($Br(\eta^{\pm} \to \ell^{\pm}N_k) \equiv Br_{\eta^{\pm}}^{\ell N_k}$) is correlated with $\tan^2\theta_{23}$. From the best fit point value ($\tan^2\theta_{23} = 1$) $Br_{\eta^{\pm}}^{\mu N_3} \simeq Br_{\eta^{\pm}}^{\tau N_3}$ is expected. Furthermore, the 3σ range for the atmospheric mixing angle allows one to predict this observable to lie within the interval [0.35,3.0], as indicated by the horizontal dashed lines in Fig. 3.

We have found that there exists an upper bound on the ratio of decay branching ratios

$$\frac{Br_{\eta^{\pm}}^{eN_3}}{Br_{\eta^{\pm}}^{\mu N_3} + Br_{\eta^{\pm}}^{\tau N_3}} \lesssim 1.2 \times 10^{-1} \tag{37}$$

derived from the correlation between this observable and $\tan^2\theta_{13}$ and demonstrated by Fig. 4. From this bound $Br_{\eta^{\pm}}^{eN_3}$

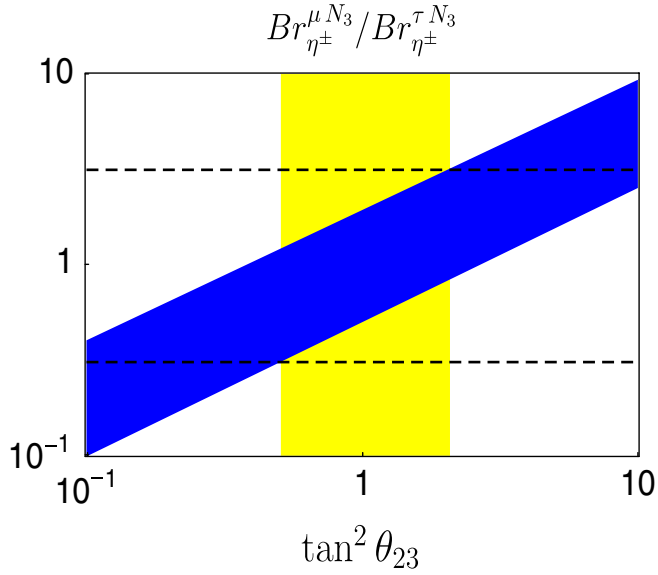

FIG. 3 (color online). Ratio of decay branching ratios $Br^{\mu N_3}_{\eta^\pm}/Br^{\tau N_3}_{\eta^\pm}$ versus $\tan^2\theta_{23}$. The vertical strip indicates the current 3σ range for $\tan^2\theta_{23}$ whereas the horizontal lines indicate the predicted range for this observable.

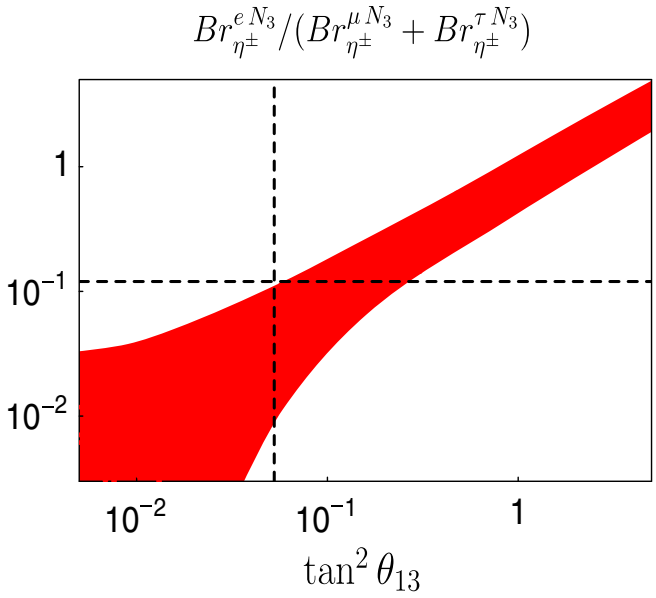

FIG. 4 (color online). Ratio of decay branching ratios $Br^{eN_3}_{\eta^\pm}/(Br^{\mu N_3}_{\eta^\pm}+Br^{\tau N_3}_{\eta^\pm})$ versus $\tan^2\theta_{13}$. The vertical line indicates the current 3σ upper bound for $\tan^2\theta_{13}$ whereas the horizontal lines indicate the predicted upper bound for this observable.

is expected to be around 1 order of magnitude smaller than $Br^{\mu N_3}_{\eta^\pm}+Br^{\tau N_3}_{\eta^\pm}$, which in turn implies, according to $Br^{\mu N_3}_{\eta^\pm}\simeq Br^{\tau N_3}_{\eta^\pm}$, that eN_3 final states are further suppressed than μN_3 and τN_3 final states.

From Eqs. (8) and (11) we found a quantity, R_-/R_+, which is related to R. $R_\mp$ can be written as

$$\frac{R_\mp}{\mathcal{R}_f}=1\mp\left[1-4r_N\frac{\sum_{i,j}Br^{\ell_i N_2}_\eta Br^{\ell_j N_3}_\eta-(\sum_i\sqrt{Br^{\ell_i N_2}_\eta Br^{\ell_i N_3}_\eta})^2}{(r_N\sum_i Br^{\ell_i N_2}_\eta+\sum_i Br^{\ell_i N_3}_\eta)^2}\right]^{1/2},\tag{38}$$

where i, j run over e, μ, τ, r_N corresponds to the right-handed neutrino mass ratio defined in Eq. (10) and $\mathcal{R}_f$ is a common global factor that involves the same parameters that define $\mathcal{G}_f$ [see Eq. (9)] and decay branching ratios. Note that in the ratio R_-/R_+ this factor cancel. Numerical results are shown in Fig. 5. The spread in the plot is due to an ambiguity in the sign of the Yukawa couplings. From the current 3σ range for $\Delta m_{12}/\Delta m_{23}$ (vertical shaded strip in Fig. 5), this quantity is predicted to lie in the range (horizontal dashed lines) $[1.4\times10^{-2}, 2.0\times10^{-1}]$.

As long as the constraints $|\mathbf{h_2}|/|\mathbf{h_3}|<1$ and $M_2/M_3<1$ are satisfied, the contributions of N_2 to the neutrino mass matrix are small in comparison with those from N_3. Thus, the atmospheric and reactor angles approximate to Eqs. (14). The results shown in Figs. 3 and 4 can be understood as a consequence of these constraints. Note that the sharpest correlations among the decay patterns of the charged scalar with neutrino mixing angles are obtained for the largest allowed (by neutrino experimental data) hierarchies between the parameter space vectors $|\mathbf{h_2}|$ and $|\mathbf{h_3}|$ and the right-handed neutrino masses M_2 and M_3.

In order to generate an inverted light neutrino mass spectrum $(\mathcal{M}_\nu)_{11}$ has to be large [of the same order of $(\mathcal{M}_\nu)_{22,33,23}$]. Thus, large contributions from the loop involving N_2 are necessary. These contributions *spoil* the leading projective nature of the neutrino mass matrix and therefore the atmospheric and reactor angles are no longer determined by Eq. (14). Accordingly, the correlations among collider observables and neutrino mixing angles we have discussed will not hold in this case. However, in principle, these results can be used to discriminate between the normal and inverted mass hierarchies as follows: If $M_3>M_2$ and $\sum_\alpha Br^{\ell_\alpha N_2}_\eta/\sum_\alpha Br^{\ell_\alpha N_3}_\eta<1$ [50] are experimentally established but none of the observables given in Figs. 3 and 4 are found to be in the range predicted by neutrino physics, the normal mass spectrum will be excluded.

$W^\pm$ final states are also possible depending on whether the mass difference $\Delta M=m_\eta-m_{R,I}$ is larger than M_W. Once kinematically open, this decay channel will dominate over the fermionic final states. However, as illustrated in Fig. 6, even in that case the fermionic decay branching

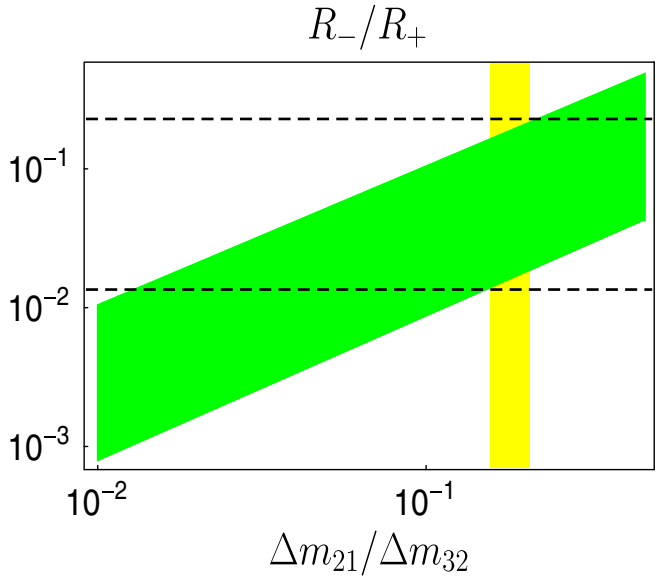

FIG. 5 (color online). Ratio of decay branching ratios R_-/R_+ versus $\Delta m_{12}/\Delta m_{23}$. The vertical shaded strip indicates the current 3σ range for $\Delta m_{12}/\Delta m_{23}$ whereas the horizontal dashed lines shows the allowed region for R_-/R_+.

ratios can be as large as $\sim 10^{-2}$. Albeit possibly problematic to be measured at LHC might be measurable at ILC. As indicated in Fig. 6 (shaded region) larger values of these branching ratios are excluded by the current upper bound on $Br(\mu \to e\gamma)$ (see the next section).

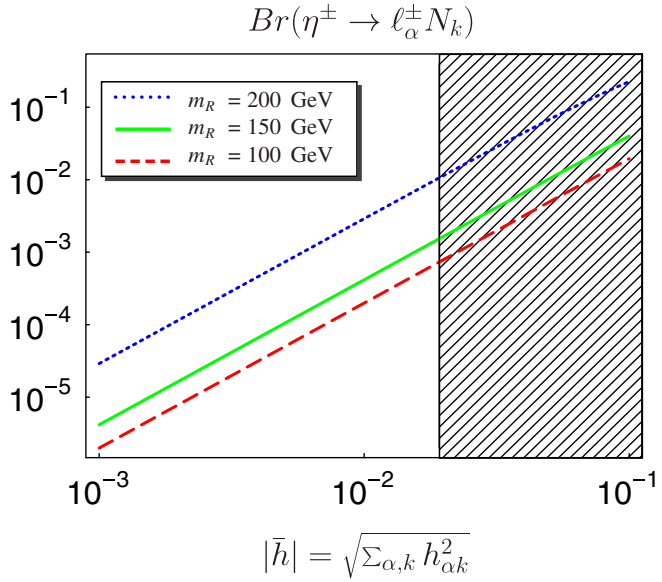

FIG. 6 (color online). Charged scalar fermionic decay branching ratio as a function of the average Yukawa coupling $|\bar{h}|$ for the case in which W gauge boson final states are kinematically open. The charged scalar mass has been fixed to 300 GeV. The shaded region is excluded by the experimental upper bound on $Br(\mu \to e\gamma)$.

VI. FLAVOR VIOLATING CHARGED LEPTON DECAYS

In this section we will derive upper bounds on the Yukawa couplings, $h_{\alpha k}$, and briefly discuss possible low-energy lepton flavor violating signals of the model. The set of Yukawa interactions induced by the right-handed neutrinos and the $SU(2)$ doublet η are responsible for lepton flavor violating radiative decays of the type $l_\alpha \to l_\beta \gamma$. Here we will concentrate on $\mu \to e\gamma$. The bounds derived from $\tau \to e\gamma$ and $\tau \to \mu\gamma$ decays are much weaker than those from $\mu \to e\gamma$ and thus we will not consider them.

In the limit $m_\beta \ll m_\alpha$ the partial decay width of $l_\alpha \to l_\beta \gamma$, induced by $\eta^\pm$ and N_k, can be written as [51]

$$\Gamma(l_\alpha \to l_\beta \gamma) = 2\alpha m_\alpha^3 \left(\frac{m_\alpha}{96\pi^2}\right)^2 \frac{|\sum_{k=1}^3 h_{\alpha k}^* h_{\beta k}|^2}{m_\eta^4}. \quad (39)$$

From the above expression the decay branching ratio for $\mu \to e\gamma$ can be written as

$$Br(\mu \to e\gamma) \simeq \frac{\Gamma(\mu \to e\gamma)}{\Gamma(\mu \to e\bar{\nu}_e \nu_\mu)} = \frac{\alpha}{24\pi G_F^2} \frac{|\sum_{k=1}^3 h_{1k}^* h_{2k}|^2}{m_\eta^4}, \quad (40)$$

and the current upper bound on this process yields the upper bound

$$\left|\sum_{k=1}^3 h_{1k}^* h_{2k}\right| \lesssim 4.1 \times 10^{-5} \left(\frac{m_\eta}{100\ \text{GeV}}\right)^2. \quad (41)$$

The largest value for these Yukawa couplings is derived from the largest charged scalar mass, $m_\eta = 400$ GeV, in this case

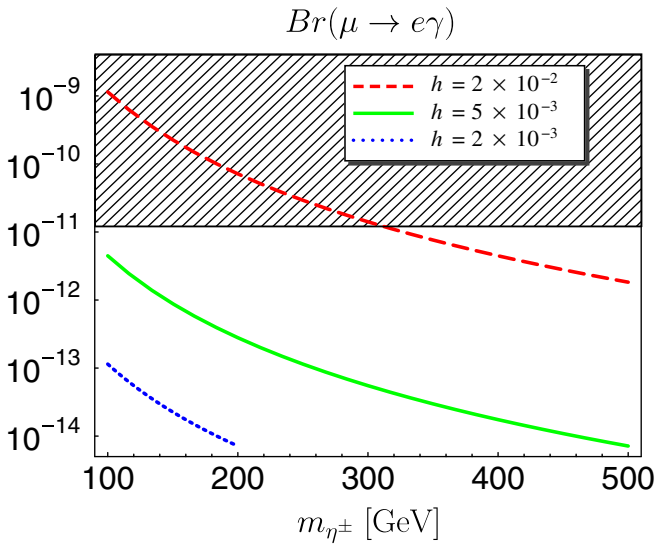

FIG. 7 (color online). $Br(\mu \to e\gamma)$ as a function of the charged scalar mass under the assumption of nonhierarchical Yukawa couplings. The shaded region is excluded by the current experimental upper bound.

$$\left| \sum_{k=1}^{3} h_{1k}^{*} h_{2k} \right| \lesssim 6.5 \times 10^{-4}. \quad (42)$$

For smaller charged scalar masses the bound becomes more stringent. Note that this constraint can be satisfied by either $h_{1k} \ll h_{2k}$ or $h_{2k} \ll h_{1k}$, an exception being the case of nonhierarchical Yukawa couplings. Under this assumption, and for $m_\eta = 300$ GeV, the upper bound $h \lesssim 1.9 \times 10^{-2}$ can be placed. This constraint corresponds to the shaded region shown in Fig. 6.

Since we do not have a theory for the Yukawas, an absolute value for $Br(\mu \to e\gamma)$ cannot be predicted. However, assuming nonhierarchical couplings this branching ratio is found to be larger than 10^{-14} for $h \gtrsim 10^{-3}$ as shown in Fig. 7. Note that this result is a consequence of the assumption $\mathcal{O}(h_{1k}) \approx \mathcal{O}(h_{2k})$ and not a general feature of the model.

VII. SUMMARY

Assuming the mass spectrum $M_1 \ll M_2 < M_3 < m_\eta$ we have studied some phenomenological aspects of the radiative seesaw model [19]. In particular, we showed that current experimental neutrino data can be used to constrain the parameter space of the model. Thus, some fermionic decays of the charged scalar $\eta^\pm$ are correlated with neutrino mixing angles which in turn allows one to predict several ratios of decay branching ratios. Especially interesting is that, if the $\eta^\pm$ is produced at colliders, a similar number of events with τ and μ final states is expected, whereas events with e are expected to be small. As has been said, these predictions could be tested in accelerator experiments depending on whether the decaying right-handed neutrino can be identified. We have discussed how this could be achieved by either counting the numbers of leptons emerging from a given vertex or by looking to the kinematic end point of the lepton pair invariant mass distribution [47].

We have found that the lightest sterile neutrino is a WDM particle which, though stable, cannot be the only DM component of the Universe. Its contribution to the DM relic density is less than 10%. Therefore, another cold DM relic must be responsible for the remaining 90%.

Finally, we have derived upper bounds on the Yukawa couplings of the model from the experimental upper limit on $Br(\mu \to e\gamma)$. We have shown that under the assumption of nonhierarchical Yukawa couplings $Br(\mu \to e\gamma)$ is found to be larger than 10^{-14} for $h \gtrsim 10^{-3}$, i.e. within the range of near future experiments [39].

ACKNOWLEDGMENTS

D. A. S. wants to thanks E. Nardi, Carlos E. Yaguna, and J. Kamenik for useful comments, and epecially to M. Hirsch for critical readings of the manuscript, for very useful suggestions, and for pointing out an error in the first version of the paper. This work was partially supported by Colciencias in Colombia under Contract No. 1115-333-18740..

[1] Q. R. Ahmad *et al.* (SNO Collaboration), Phys. Rev. Lett. **89**, 011301 (2002).
[2] Y. Fukuda *et al.* (Super-Kamiokande Collaboration), Phys. Rev. Lett. **81**, 1562 (1998).
[3] K. Eguchi *et al.* (KamLAND Collaboration), Phys. Rev. Lett. **90**, 021802 (2003).
[4] D. N. Spergel *et al.* (WMAP Collaboration), Astrophys. J. Suppl. Ser. **170**, 377 (2007).
[5] P. Minkowski, Phys. Lett. **67B**, 421 (1977); T. Yanagida, in *KEK Lectures*, edited by O. Sawada and A. Sugamoto (KEK, Ibaraki, Japan, 1979); M. Gell-Mann, P. Ramond, and R. Slansky, in *Supergravity*, edited by P. van Niewenhuizen and D. Freedman (North-Holland, Amsterdam, 1979); R. N. Mohapatra and G. Senjanovic, Phys. Rev. Lett. **44**, 912 (1980); J. Schechter and J. W. F. Valle, Phys. Rev. D **22**, 2227 (1980).
[6] M. Hirsch and J. W. F. Valle, New J. Phys. **6**, 76 (2004); M. Hirsch, M. A. Diaz, W. Porod, J. C. Romao, and J. W. F. Valle, Phys. Rev. D **62**, 113008 (2000); **65**, 119901(E) (2002).
[7] M. Hirsch, A. Vicente, and W. Porod, Phys. Rev. D **77**, 075005 (2008).
[8] J. Garayoa and T. Schwetz, J. High Energy Phys. 03 (2008) 009.
[9] A. Zee, Phys. Lett. **93B**, 389 (1980); **95B**, 461 (1980); D. Aristizabal Sierra and D. Restrepo, J. High Energy Phys. 08 (2006) 036.
[10] A. Zee, Nucl. Phys. **B264**, 99 (1986); K. S. Babu, Phys. Lett. B **203**, 132 (1988); K. S. Babu and C. Macesanu, Phys. Rev. D **67**, 073010 (2003); D. Aristizabal Sierra and M. Hirsch, J. High Energy Phys. 12 (2006) 052; M. Nebot, J. F. Oliver, D. Palao, and A. Santamaria, Phys. Rev. D **77**, 093013 (2008).
[11] D. Aristizabal Sierra, M. Hirsch, and S. G. Kovalenko, Phys. Rev. D **77**, 055011 (2008); U. Mahanta, Phys. Rev. D **62**, 073009 (2000).
[12] S. Hannestad and G. Raffelt, J. Cosmol. Astropart. Phys. 04 (2004) 008; P. Crotty, J. Lesgourgues, and S. Pastor, Phys. Rev. D **69**, 123007 (2004).
[13] Models where all dark matter is hot are ruled out completely by current cosmological data.
[14] J. R. Primack, arXiv:astro-ph/9707285.
[15] P. Bode, J. P. Ostriker, and N. Turok, Astrophys. J. **556**, 93 (2001); B. Moore, T. Quinn, F. Governato, J. Stadel, and

G. Lake, Mon. Not. R. Astron. Soc. **310**, 1147 (1999); V. Avila-Reese, P. Colin, O. Valenzuela, E. D'Onghia, and C. Firmani, Astrophys. J. **559**, 516 (2001).
[16] M. Viel, J. Lesgourgues, M. G. Haehnelt, S. Matarrese, and A. Riotto, Phys. Rev. D **71**, 063534 (2005); M. Viel, G. D. Becker, J. S. Bolton, M. G. Haehnelt, M. Rauch, and W. L. W. Sargent, Phys. Rev. Lett. **100**, 041304 (2008).
[17] In this case WDM gives a contribution of $\sim$10% to the total DM relic density [16].
[18] J. Kubo and D. Suematsu, Phys. Lett. B **643**, 336 (2006); M. Lattanzi and J. W. F. Valle, Phys. Rev. Lett. **99**, 121301 (2007); C. Boehm, Y. Farzan, T. Hambye, S. Palomares-Ruiz, and S. Pascoli, Phys. Rev. D **77**, 043516 (2008); C. Arina, F. Bazzocchi, N. Fornengo, J. C. Romao, and J. W. F. Valle, Phys. Rev. Lett. **101**, 161802 (2008); E. Ma, Phys. Lett. B **662**, 49 (2008).
[19] E. Ma, Phys. Rev. D **73**, 077301 (2006).
[20] J. Kubo, E. Ma, and D. Suematsu, Phys. Lett. B **642**, 18 (2006).
[21] G. Passarino and M. J. G. Veltman, Nucl. Phys. **B160**, 151 (1979).
[22] We will denote the $\eta^{\pm}$ mass by m_{η}.
[23] A suppression mechanism based on a low-energy flavor symmetry in the same type of models, with a radiative neutrino mass generation, was proposed in [24].
[24] Y. Kajiyama, J. Kubo, and H. Okada, Phys. Rev. D **75**, 033001 (2007).
[25] S. Dodelson and L. M. Widrow, Phys. Rev. Lett. **72**, 17 (1994).
[26] T. Asaka, M. Laine, and M. Shaposhnikov, J. High Energy Phys. 01 (2007) 091.
[27] A possible origin of this symmetry was discussed in [18].
[28] A. D. Dolgov and S. H. Hansen, Astropart. Phys. **16**, 339 (2002).
[29] K. Abazajian, G. M. Fuller, and W. H. Tucker, Astrophys. J. **562**, 593 (2001).
[30] M. Mapelli, A. Ferrara, and E. Pierpaoli, Mon. Not. R. Astron. Soc. **369**, 1719 (2006).
[31] A. Boyarsky, A. Neronov, O. Ruchayskiy, and M. Shaposhnikov, Mon. Not. R. Astron. Soc. **370**, 213 (2006); JETP Lett. **83**, 133 (2006); A. Boyarsky, D. Iakubovskyi, O. Ruchayskiy, and V. Savchenko, Mon. Not. R. Astron. Soc. **387**, 1361 (2008).
[32] If the sterile neutrinos as WDM are generated in decays of some heavier particles, then the situation may change [33].
[33] A. Kusenko, Phys. Rev. Lett. **97**, 241301 (2006); K. Petraki and A. Kusenko, Phys. Rev. D **77**, 065014 (2008); K. Petraki, Phys. Rev. D **77**, 105004 (2008); D. Boyanovsky, Phys. Rev. D **78**, 103505 (2008).
[34] U. Seljak, A. Makarov, P. McDonald, and H. Trac, Phys. Rev. Lett. **97**, 191303 (2006).
[35] M. Viel, J. Lesgourgues, M. G. Haehnelt, S. Matarrese, and A. Riotto, Phys. Rev. Lett. **97**, 071301 (2006).
[36] D. Gorbunov, A. Khmelnitsky, and V. Rubakov, J. Cosmol. Astropart. Phys. 10 (2008) 041.
[37] A. Palazzo, D. Cumberbatch, A. Slosar, and J. Silk, Phys. Rev. D **76**, 103511 (2007).
[38] We have assumed that at T_D only N_1, among N_k's, remains relativistic.
[39] "MEG experiment." Home page: http://meg.web.psi.ch/index.html.
[40] A. Djouadi, Phys. Rep. **459**, 1 (2008).
[41] Q. H. Cao, E. Ma, and G. Rajasekaran, Phys. Rev. D **76**, 095011 (2007).
[42] M. Battaglia, A. Ferrari, A. Kiiskinen, and T. Maki, arXiv: hep-ex/0112015.
[43] F. de Campos, O. J. P. Eboli, M. B. Magro, W. Porod, D. Restrepo, M. Hirsch, and J. W. F. Valle, J. High Energy Phys. 05 (2008) 048; D. Aristizabal Sierra, W. Porod, D. Restrepo, and C. E. Yaguna, Phys. Rev. D **78**, 015015 (2008).
[44] Scalar masses are also constrained from the requirement of scalar production at LHC or ILC (upper bound) and from LEP data (lower bound).
[45] M. Maltoni, T. Schwetz, M. A. Tortola, and J. W. F. Valle, New J. Phys. **6**, 122 (2004). Online version 6 in arXiv:hep-ph/0405172 contains updated fits with data included up to Sep 2007.
[46] R. M. Barnett, J. F. Gunion, and H. E. Haber, Phys. Lett. B **315**, 349 (1993).
[47] B. C. Allanach, C. G. Lester, M. A. Parker, and B. R. Webber, J. High Energy Phys. 09 (2000) 004; K. Kawagoe, M. M. Nojiri, and G. Polesello, Phys. Rev. D **71**, 035008 (2005); B. K. Gjelsten, D. J. Miller, and P. Osland, J. High Energy Phys. 12 (2004) 003; D. J. Miller, P. Osland, and A. R. Raklev, J. High Energy Phys. 03 (2006) 034.
[48] The charged scalar mass was also taken in this range.
[49] M_1 was taken below 16 eV as required by DM constraints.
[50] This relation is derived from the constraint $|\mathbf{h_2}|/|\mathbf{h_3}| < 1$.
[51] Note that we are considering the case $M_k^2 \ll m_{\eta}^2$ and therefore the loop function reduces to a factor of $1/6$.